Supplemental materials

Deterministic *N*-photon State Generation Using Lithium Niobate on Insulator Device

Hua-Ying Liu[a, †], Minghao Shang[a, †], Xiaoyi Liu[a], Ying Wei[a], Minghao Mi[a], Lijian Zhang[a], Yan-Xiao Gong[a, *], Zhenda Xie[a, *], And Shi-Ning Zhu[a]

[a]National Laboratory of Solid State Microstructures, School of Electronic Science and Engineering, School of Physics, College of Engineering and Applied Sciences, and Collaborative Innovation Center of Advanced Microstructures, Nanjing University, Nanjing 210093, China

*****Address all correspondence to Yan-Xiao Gong, E-mail: gongyanxiao@nju.edu.cn; Zhenda Xie, E-mail: xiezhenda@nju.edu.cn

[†]These authors contributed equally to this work.

A. The Hamiltonian of the Microring-bus system

First, we calculate the process of deterministic parametric down-conversion (DPDC) in the periodically poled lithium niobate on insulator (PPLNOI) microring resonator. We model the DPDC process using the cavity-enhanced dual potential operators $\hat{\Lambda}(z,t)$ for quantization of the electromagnetic field, and the Hamiltonian can be written as the sum of linear ($\hat{H}_{\mathrm{L}}$) and nonlinear ($\hat{H}_{\mathrm{NL}}$) terms: [45, 46]

$$\begin{aligned}\hat{H} &= \hat{H}_{\mathrm{NL}} + \hat{H}_{\mathrm{L}} \\ &= \frac{A_{\mathrm{eff}}}{3}\cdot\left(\frac{-\chi^{(2)}}{\varepsilon_0^2 n_p^2 n_s^2 n_i^2}\right)\int_L \mathrm{d}z \frac{\partial\hat{\Lambda}_s}{\partial z}\frac{\partial\hat{\Lambda}_i}{\partial z}\frac{\partial\hat{\Lambda}_p}{\partial z} + \sum_{j=p,s,i}\frac{A_j}{2}\int_L \mathrm{d}z\left[\frac{1}{\varepsilon_0 n_j^2}\left(\frac{\partial\hat{\Lambda}_j}{\partial z}\right)^2 + \mu_0\left(\frac{\partial\hat{\Lambda}_j}{\partial t}\right)^2\right].\end{aligned} \quad \text{(S1)}$$

where j = p, s, and i represent pump, signal and idler, respectively. $A_{\mathrm{eff}} \equiv \iint_S \mathrm{d}x\mathrm{d}y U_p(x,y)U_s^*(x,y)U_i^*(x,y)$ is the effective spatial overlap, and $A_j \equiv \iint \mathrm{d}x\mathrm{d}y\left|U_j(x,y)\right|^2$ is the mode area for photon j, with S denoting cross-section of the waveguide and $U(x, y)$ denoting the normalized transverse mode distribution of electrical field.

And L, n_j correspond to the length of the microring resonator and the effective refractive index of photon j, respectively.

Here, $\hat{\Lambda}_j(z,t)$ is achieved using the "modes of the universe approach" in Ref. 45, with

$$\hat{\Lambda}_j(z,t) = \int_0^\infty \mathrm{d}k_j \frac{1}{ik_j^{3/2}} \cdot \left(\hat{a}_{k_j} e^{-i\omega_j t} D_{k_j}(z) - h.c.\right), \tag{S2}$$

where $D_{k_j}(z)e^{-i\omega_j t} = ik_j\sqrt{\hbar n_j / (2\mu_0 c A_j)} \cdot u_{k_j}(z)e^{-i\omega_j t}$ represents the electric displacement field of wave vector k_j in the propagation direction (ignoring transmission loss) in the microring resonator, with the cavity enhancement effect reflected in the coefficient of $u_{k_j}(z)$. t is the evolution time, $\hat{a}_{k_j}$ stands for the photon annihilation operator of mode k_j, ω_j is the angular frequency, and *h.c.* represents the Hermitian conjugate. As shown in Fig. 2(c) in the main text, for the microring resonator with a length of L, u_{k_j} can be written as

$$u_{k_j}(z) = \begin{cases} \beta_{k_j} e^{ik_j z} & (z < 0), \\ \alpha_{k_j} e^{ik_j z} & (0 \le z < L), \\ \gamma_{k_j} e^{ik_j z} & (z \ge L), \end{cases} \tag{S3}$$

where $z \in [0, L)$ represents coordinates in the resonator, and the coordinates of the coupling point between the bus waveguide and the microring resonator before and after coupling are $z = 0$, and $z = L$, respectively.

According to the boundary conditions at $z = 0$ and $z = L$, we can obtain:

$$\begin{cases} \beta_{k_j} e^{ik_j \cdot 0} = i\sqrt{T}\alpha_{k_j} e^{ik_j \cdot 0} + \sqrt{1-T}\gamma_{k_j} e^{ik_j \cdot L}, \\ \alpha_k e^{ik_j \cdot L} = i\sqrt{T}\gamma_{k_j} e^{ik_j \cdot L} + \sqrt{1-T}\alpha_{k_j} e^{ik_j \cdot 0}, \end{cases} \tag{S4}$$

where T is the transmittance of the coupling between the bus and the microring resonator. Substituting the orthogonal relation of the longitudinal modes [45] $\int_{-\infty}^{\infty} u_{k_{j1}}^*(z) u_{k_{j2}}(z) \mathrm{d}z = \delta(k_{j1} - k_{j2})$ in to Eq. (S4), we can get

$$\begin{cases} \alpha_{k_j} = \dfrac{1}{\sqrt{2\pi}} \dfrac{i\sqrt{T}}{1-\sqrt{1-T}e^{-ik_jL}}, \\ \beta_{k_j} = \dfrac{1}{\sqrt{2\pi}} \dfrac{\sqrt{1-T}e^{ik_jL}-1}{1-\sqrt{1-T}e^{-ik_jL}}, \end{cases} \tag{S5}$$

where α_{k_j} reflects the enhancement effect of the resonator on the mode.

Substituting Eq. (S5) into Eq. (S2), we can finally obtain

$$\hat{\Lambda}_j(z,t) = \int_0^\infty \mathrm{d}k_j \sqrt{\frac{\hbar}{2\mu_0\omega_j A_j}} \cdot \left(\alpha_{k_j}\hat{a}_{k_j} e^{ik_j z} e^{-i\omega_j t} + h.c.\right). \tag{S6}$$

After substituting Eq. (S6) into Eq. (S1) and using the rotating wave approximation, [45, 47] the Hamiltonian can be derived as

$$\begin{aligned} \hat{H} &= \hat{H}_{\mathrm{NL}} + \hat{H}_{\mathrm{L}} \\ &= \frac{-1}{3}\left(\frac{\hbar}{4\pi\mu_0 c}\right)^{\frac{3}{2}} \int_L \mathrm{d}z \int_0^\infty \mathrm{d}k_p \int_0^\infty \mathrm{d}k_s \int_0^\infty \mathrm{d}k_i \frac{A_{\mathrm{eff}}}{\sqrt{A_p A_s A_i}} \sqrt{n_p n_s n_i}\sqrt{k_p k_s k_i} \\ &\cdot\left(\eta^{(2)} \frac{\sqrt{T_p}}{1-\sqrt{1-T_p}e^{-ik_pL}} \frac{\sqrt{T_s}}{1-\sqrt{1-T_s}e^{ik_sL}} \frac{\sqrt{T_i}}{1-\sqrt{1-T_i}e^{ik_iL}} e^{i(k_p-k_s-k_i)z} e^{-i(\omega_p-\omega_s-\omega_i)t} \hat{a}_{k_s}^{+}\hat{a}_{k_i}^{+}\hat{a}_{k_p} + h.c.\right) \\ &+ \sum_{j=p,s,i} \int_0^\infty \mathrm{d}k_j \frac{\hbar c k_j L}{2\pi n_j} \frac{T_j}{2-T_j-2\sqrt{1-T_j}\cos\left(k_j L\right)} \hat{a}_{k_j}^{+}\hat{a}_{k_j}, \end{aligned} \tag{S7}$$

Here we use the second-order nonlinear susceptibility $\chi^{(2)} = \chi_{\mathrm{eff}}^{(2)} \cdot e^{-iGz}$ to simplify the Hamiltonian, where $\chi_{\mathrm{eff}}^{(2)}$ is the effective second-order nonlinear coefficient, and G is the reciprocal lattice vector provided by periodically poled structure and perform the integral over z in the range of (0, L). Thus, the Hamiltonian is deduced as

$$\begin{aligned} \hat{H} &= \hat{H}_{\mathrm{NL}} + \hat{H}_{\mathrm{L}} \\ &= \frac{\chi_{\mathrm{eff}}^{(2)}}{3\sqrt{\varepsilon_0}}\left(\frac{\hbar c}{4\pi}\right)^{\frac{3}{2}} \int_0^\infty \mathrm{d}k_p \int_0^\infty \mathrm{d}k_s \int_0^\infty \mathrm{d}k_i \left(\frac{1}{n_p n_s n_i}\right)^{\frac{3}{2}} \frac{A_{\mathrm{eff}}}{\sqrt{A_p A_s A_i}} \sqrt{k_p k_s k_i} L \mathrm{sinc}\left(\frac{\left(k_p-k_s-k_i-G\right)L}{2}\right) \\ &\cdot\left(\frac{\sqrt{T_p}}{1-\sqrt{1-T_p}e^{-ik_pL}} \frac{\sqrt{T_s}}{1-\sqrt{1-T_s}e^{ik_sL}} \frac{\sqrt{T_i}}{1-\sqrt{1-T_i}e^{ik_iL}} e^{i\frac{(k_p-k_s-k_i-G)L}{2}} e^{-i(\omega_p-\omega_s-\omega_i)t} \hat{a}_{k_s}^{+}\hat{a}_{k_i}^{+}\hat{a}_{k_p} + \mathrm{h.c.}\right) \\ &+ \sum_{j=p,s,i} \int_0^\infty \mathrm{d}k_j \frac{\hbar c k_j L}{2\pi n_j} \frac{T_j}{2-T_j-2\sqrt{1-T_j}\cos\left(k_j L\right)} \hat{a}_{k_j}^{+}\hat{a}_{k_j}. \end{aligned} \tag{S8}$$

B. The conditions for Single-longitude-mode (SLM) oscillation in PDC process

To have unbroadened spectra for *N*-photon state generation, single-longitude-mode (SLM) oscillation must be achieved in this cavity-enhanced case, which requires the difference of the free spectrum range (FSR) of signal and idler light to be larger than linewidth of the cavity resonances. [48, 49] Assuming triple-resonance PDC condition is satisfied at $\omega_{p0} = \omega_{s0} + \omega_{i0}$, with $n_{j0} L \omega_{j0} = 2\pi N_j c$ for j = p, s, and i, where N_j is a positive integer. Hence the frequency of the $m_{s(i)}$th sideband resonance modes aside from the center signal and idler modes are,

$$\omega_{s0(i0),\pm m_{s(i)}} = \omega_{s0(i0)} \pm m_{s(i)} \Delta\Omega_{s(i)}, \tag{S9}$$

where $\Delta\Omega_{s(i)}$ indicates the FSR of angular frequency for signal and idler, respectively, and $m_{s(i)}$ are positive integers. If PDC process can happen at $m_s = -m_i \equiv m$ sideband resonance modes for signal and idler, respectively, the energy conservation condition requires

$$\left| m\Delta\Omega_s - m\Delta\Omega_i \right| < \Delta\omega, \tag{S10}$$

where $\Delta\omega \equiv \omega / Q$ is the angular frequency bandwidth of the resonance modes. Although energy conservation condition may also be satisfied when $m_s \neq -m_i$, with $\left| m_s \Delta\Omega_s - m_i \Delta\Omega_i \right| < \Delta\omega$, we only discuss the case for $m_s = -m_i$ here. Because when $m_s \neq -m_i$, the phase mismatch $\Delta k_{\text{mis}} = 2\pi \left| m_s - m_i \right| / L \geq 2\pi / L$ is larger than the phase matching bandwidth of the wave vector $\Delta k_{\text{QPM}} \approx 5.56 / L$, hence PDC will not happen under such condition.

According to Eq. (S10), to achieve SLM oscillation, it requires

$$\left| \Delta\Omega_{s0} - \Delta\Omega_{i0} \right| > \Delta\omega, \tag{S11}$$

where $\Delta\Omega_{s0(i0)}$ is the FSR of the nearest neighbor resonance sideband of ω_{s0} and ω_{i0}, which can be approximately treat as $\Delta\Omega_{s0(i0)} \approx 2\pi c/n_{s0(i0)}L$. Substituting the expression of $\Delta\Omega_{s0(i0)}$ and $\Delta\omega$ in to Eq. (S11), the Q requirement can be derived as

$$Q > \frac{\omega R}{c\left|1/n_{s0} - 1/n_{i0}\right|}, \tag{S12}$$

where R is the radius of the microring, with $L = 2\pi R$.

C. The Hamiltonian for high-Q Microring-bus system

In this section, we calculate and simplify the Hamiltonian for high-Q microring-bus system under SLM oscillation condition. For a high-Q microring resonator, its resonant modes bandwidth $\Delta\omega = \omega/Q$ is much smaller than its free spectrum range (FSR) $\Delta\Omega_j = 2\pi c/n_j L = c/n_j R$, where R is the radius of the microring resonator, $j = p, s, i$. Therefore, for SLM oscillation PDC process, the integral range of k_j can be safely replaced from $(0, +\infty)$ to $\left(k_{j0} - \Delta, k_{j0} + \Delta\right)$, where k_{j0} is the wave vector at the center and $\Delta \equiv 1/2\pi R$. Here, the integral of k_p, k_s, and k_i are written as $\int_{k_{p0}-\Delta}^{k_{p0}+\Delta}$, $\int_{k_{s0}-\Delta}^{k_{s0}+\Delta}$ and $\int_{k_{i0}-\Delta}^{k_{i0}+\Delta}$ in the following text, respectively.

Within this range, k_j, n_j and A_{eff} can be approximately regarded as constants at center frequencies (represented by the subscript 0). For triple-resonant PDC processes in high-Q resonators, the wave vector bandwidth of the parametric fields is approximately equal to that of resonance modes, which is $\Delta k_j \equiv k_{j0}/Q$. It is much smaller than the full width at half maximum (FWHM) bandwidth $\Delta k_{\text{QPM}} \approx 2.78/\pi R$ of $\text{sinc}^2\left(\left(k_p - k_s - k_i - G\right)L/2\right)$ (for example, when $Q = 10^7$, $R = 30$ μm with the wavelength at 1310 nm, $\Delta k_{\text{QPM}} \approx 3\times10^4 \cdot \Delta k_j$). Hence

it can be simplified as $\mathrm{sinc}\left(\left(k_p-k_s-k_i-G\right)L/2\right)\approx 1$. Therefore, the Hamiltonian can be rewritten as

$$\begin{aligned}\frac{\hat{H}}{\hbar}&=\frac{\hat{H}_{\mathrm{NL}}}{\hbar}+\frac{\hat{H}_{\mathrm{L}}}{\hbar}\\&=g\int_{k_{p0}-\Delta}^{k_{p0}+\Delta}\mathrm{d}k_p\int_{k_{s0}-\Delta}^{k_{s0}+\Delta}\mathrm{d}k_s\int_{k_{i0}-\Delta}^{k_{i0}+\Delta}\mathrm{d}k_i\left(v\left(k_p\right)v^*\left(k_s\right)v^*\left(k_i\right)\hat{a}_{k_s}^{+}\hat{a}_{k_i}^{+}\hat{a}_{k_p}e^{-i\left(\omega_p-\omega_s-\omega_i\right)t}+h.c.\right)\\&+\frac{ck_{p0}R}{n_{p0}}\int_{k_{p0}-\Delta}^{k_{p0}+\Delta}\mathrm{d}k_p\left|v\left(k_p\right)\right|^2\hat{a}_{k_p}^{+}\hat{a}_{k_p}+\frac{ck_{s0}R}{n_{s0}}\int_{k_{s0}-\Delta}^{k_{s0}+\Delta}\mathrm{d}k_s\left|v\left(k_s\right)\right|^2\hat{a}_{k_s}^{+}\hat{a}_{k_s}+\frac{ck_{i0}R}{n_{i0}}\int_{k_{i0}-\Delta}^{k_{i0}+\Delta}\mathrm{d}k_i\left|v\left(k_i\right)\right|^2\hat{a}_{k_i}^{+}\hat{a}_{k_i},\end{aligned}\tag{S13}$$

where

$$g\equiv\frac{\chi_{\mathrm{eff}}^{(2)}}{12}\sqrt{\frac{\hbar}{\varepsilon_0\pi}}\cdot\left(\frac{c}{n_{p_0}n_{s_0}n_{i_0}}\right)^{3/2}\cdot\frac{A_{\mathrm{eff}}}{\sqrt{A_{p_0}A_{s_0}A_{i_0}}}\sqrt{k_{p_0}k_{s_0}k_{i_0}}R,\tag{S14}$$

$$v\left(k_j\right)\equiv\frac{\sqrt{T_j}}{1-\sqrt{1-T_j}e^{-ik_j\cdot 2\pi R}}.\tag{S15}$$

To simplify the Hamiltonian, we define a new operator $\hat{\zeta}_j\equiv\int_{k_{j0}-\Delta}^{k_{j0}+\Delta}\mathrm{d}k_j v\left(k_j\right)\hat{a}_{k_j}$, whose commutation relation is

$$\left[\hat{\zeta}_j,\hat{\zeta}_j^{+}\right]=\int_{k_{j0}-\Delta}^{k_{j0}+\Delta}\mathrm{d}k_j\left|v\left(k_j\right)\right|^2=\int_{k_{j0}-\Delta}^{k_{j0}+\Delta}\mathrm{d}k_j\frac{T_j}{2-T_j-2\sqrt{1-T_j}\cos\left(2\pi k_jR\right)},\tag{S16}$$

Since Δk_j is extremely narrow in the case of high *Q*, i.e. $\Delta k_j\ll k_{j0}$, we can take Taylor expansion of $\cos\left(2\pi k_jR\right)$ to the first order at k_{j0}:

$$\left[\hat{\zeta}_j,\hat{\zeta}_j^{+}\right]=\int_{k_{j0}-\Delta}^{k_{j0}+\Delta}\mathrm{d}k_j\frac{T_j}{2-T_j-2\sqrt{1-T_j}\left\{1-\left[2\pi\left(k_j-k_{j0}\right)R^2\right]/2\right\}},\tag{S17}$$

After integration, we obtain

$$\left[\hat{\zeta}_j,\hat{\zeta}_j^{+}\right]=\frac{T_j}{2\left(1-T_j\right)^{\frac{1}{4}}\left(1-\sqrt{1-T_j}\right)\cdot R}.\tag{S18}$$

For high-*Q* microring resonators, $T\ll 1$, hence we can take Taylor expansion of $T_j/\left[\left(1-T_j\right)^{1/4}\left(1-\sqrt{1-T_j}\right)\right]$ to the second order at $T=0$, and get $\left[\hat{\zeta}_j,\hat{\zeta}_j^{+}\right]\approx 1/R$. Naturally, we can define the "normalized discrete Hilbert-space photon annihilation operator" $\hat{\zeta}_j\equiv\sqrt{R}\hat{\zeta}_j$, which

satisfies the commutation relation $\left[\hat{\varsigma}_j,\hat{\varsigma}_j^+\right]=1$. Considering the energy conservation condition $e^{-i\left(\omega_p-\omega_s-\omega_i\right)t}=1$, the Hamiltonian can be finally simplified as

$$\frac{\hat{H}}{\hbar}=\xi\left(\hat{\varsigma}_s^+\hat{\varsigma}_i^+\hat{\varsigma}_p+\hat{\varsigma}_p^+\hat{\varsigma}_s\hat{\varsigma}_i\right)+\omega_{p0}\hat{\varsigma}_p^+\hat{\varsigma}_p+\omega_{s0}\hat{\varsigma}_s^+\hat{\varsigma}_s+\omega_{i0}\hat{\varsigma}_i^+\hat{\varsigma}_i, \tag{S19}$$

where

$$\xi\equiv g/R^{3/2}=\frac{\chi^{(2)}}{12}\sqrt{\frac{\hbar}{\pi\varepsilon_0 R}}\left(\frac{c}{n_{p_0}n_{s_0}n_{i_0}}\right)^{3/2}\frac{A_{\text{eff}}}{\sqrt{A_{p_0}A_{s_0}A_{i_0}}}\sqrt{k_{p_0}k_{s_0}k_{i_0}}. \tag{S20}$$

represents the nonlinear interaction strength.

D. Time evolution of quantum state inside high-*Q* microring resonator system

Here we use stationary Schrödinger equation to calculate the time evolution of quantum states inside the microring, where the eigenvalue equation of the Hamiltonian can be written as

$$\frac{\hat{H}}{\hbar}\left|\varphi_\lambda\right\rangle=\Lambda\left|\varphi_\lambda\right\rangle. \tag{S21}$$

Here, $\Lambda=\lambda/\hbar$. Basing on the Hamiltonian of Eq. (S19), for the initial single-photon pump state $\left|1\right\rangle_p=\hat{\varsigma}_p^\dagger\left|0\right\rangle$, its evolution is limited between the pump state $\left|1\right\rangle_p$ and down-conversion photon-pair state $\left|1,1\right\rangle_{s,i}=\hat{\varsigma}_s^\dagger\hat{\varsigma}_i^\dagger\left|0\right\rangle$. Therefore, the eigenstate can be written as

$$\left|\varphi_\lambda\right\rangle=\left(c_\lambda\hat{\varsigma}_p^+ + d_\lambda\hat{\varsigma}_s^+\hat{\varsigma}_i^+\right)\left|0\right\rangle. \tag{S22}$$

Substitute Eq. (S19) and (S22) into Eq. (S21), we can get

$$\begin{cases}\Lambda c_\lambda=\omega_{p0}c_\lambda+\xi d_\lambda,\\ \Lambda d_\lambda=\xi c_\lambda+\left(\omega_{s0}+\omega_{i0}\right)d_\lambda,\end{cases} \tag{S23}$$

Solving these equations, we can obtain

$$\Lambda_1=\omega_{p0}+\xi,\Lambda_2=\omega_{p0}-\xi. \tag{S24}$$

According to the normalized condition $\left\langle \varphi_{\lambda_1} \middle| \varphi_{\lambda_2} \right\rangle = \delta_{1,2}$, we can get $\left|c_\lambda\right|^2 + \left|d_\lambda\right|^2 = 1$. Substituting this relation to Eq. (S23), we can get $\left|c_{\lambda_1}\right|^2 = \left|c_{\lambda_2}\right|^2 = 1/2, \left|d_{\lambda_1}\right|^2 = \left|d_{\lambda_2}\right|^2 = 1/2$.

Then we can rewrite the input pump state using the base vectors,

$$\begin{aligned} \left|1\right\rangle_p &= \sum_{j=1,2} \left\langle \varphi_{\lambda_j} \middle| p \right\rangle \left| \varphi_{\lambda_j} \right\rangle \\ &= \left(\left|c_{\lambda_1}\right|^2 \hat{\varsigma}_p^+ + c_{\lambda_1}^* d_{\lambda_1} \hat{\varsigma}_s^+ \hat{\varsigma}_i^+ \right) \left|0\right\rangle + \left(\left|c_{\lambda_2}\right|^2 \hat{\varsigma}_p^+ + c_{\lambda_2}^* d_{\lambda_2} \hat{\varsigma}_s^+ \hat{\varsigma}_i^+ \right) \left|0\right\rangle \\ &= \left[\left(\left|c_{\lambda_1}\right|^2 \hat{\varsigma}_p^+ + c_{\lambda_1}^* d_{\lambda_1} \hat{\varsigma}_s^+ \hat{\varsigma}_i^+ \right) + \left(\left|c_{\lambda_2}\right|^2 \hat{\varsigma}_p^+ + c_{\lambda_2}^* d_{\lambda_2} \hat{\varsigma}_s^+ \hat{\varsigma}_i^+ \right) \right] \left|0\right\rangle. \end{aligned} \tag{S25}$$

The time evolution of the coefficient of the single-photon term is $\left|c_{\lambda_1}\right|^2 e^{-i\Lambda_1 t} + \left|c_{\lambda_2}\right|^2 e^{-i\Lambda_2 t}$. Therefore, the population of pump photons that evolve over time is [47]

$$N_p(t) = \left| \left|c_{\lambda_1}\right|^2 e^{-i\Lambda_1 t} + \left|c_{\lambda_2}\right|^2 e^{-i\Lambda_2 t} \right|^2 = \left| \frac{1}{2} \left(e^{-i\Lambda_1 t} + e^{-i\Lambda_2 t} \right) \right|^2 = \cos^2(\xi t). \tag{S26}$$

Thus, the PDC conversion efficiency from the single-photon state to the two-photon state is $\eta = \sin^2(\xi t)$, where t is the equivalent evolution time of the photon in the microring resonator.

From Eq. (S25), we can also obtain $c_{\lambda_1}^* d_{\lambda_1} + c_{\lambda_2}^* d_{\lambda_2} = 0$. Therefore, the output state evolving with time is

$$\begin{aligned} \left|\Psi(t)\right\rangle &= \left[\left(\frac{1}{2} \hat{\varsigma}_p^+ - \frac{1}{2} \hat{\varsigma}_s^+ \hat{\varsigma}_i^+ \right) e^{-i(\omega_{p0} - \xi)t} + \left(\frac{1}{2} \hat{\varsigma}_p^+ + \frac{1}{2} \hat{\varsigma}_s^+ \hat{\varsigma}_i^+ \right) e^{-i(\omega_{p0} + \xi)t} \right] \left|0\right\rangle \\ &= \left(\hat{\varsigma}_p^+ \cos(\xi t) - i \hat{\varsigma}_s^+ \hat{\varsigma}_i^+ \sin(\xi t) \right) e^{-i\omega_{p0} t} \left|0\right\rangle. \end{aligned} \tag{S27}$$

It shows that the output photon state will undergo Rabi oscillation between the single-photon and two-photon states.

E. Calculation with specific parameters for DPDC and DPUC

We use the commercial software Lumerical Mode Solutions [56] to calculate the parameters of LNOI device for DPDC and DPUC. The radius of the microring resonator for DPDC here is

30 μm, and an etched trapezoidal waveguide parameter with a top width of 0.35 μm, height of 450 nm, with 60° wall slope and 2-μm-thick SiO_2 covered was used, in which a triple-resonance PDC process of 646.91 nm→1276.80 nm + 1311.29 nm can be achieved. The mode distribution and overlap of the three wavelengths are shown in Fig. S1, and the calculated parameters results are written as follows:

$$\begin{aligned}
\chi_{\text{eff}}^{(2)} &= \frac{2}{\pi} d_{33} = \frac{2}{\pi} \times 27 \times 10^{-12}\ \text{m / V}, \\
n_{646.91} &= 2.059200,\ n_{1276.80} = 1.727274,\ n_{1311.29} = 1.711325, \\
\hbar &= 1.054572 \times 10^{-34}\ \text{J}\cdot\text{s},\ \varepsilon_0 = 8.854188 \times 10^{-12}\ \text{F / m}, \\
L &= 2\pi \times 30 \times 10^{-6}\ \text{m}, \\
\omega_{646.91} &= 2.911768 \times 10^{15}\ \text{s}^{-1},\ \omega_{1276.80} = 1.475291 \times 10^{15}\ \text{s}^{-1},\ \omega_{1311.29} = 1.436487 \times 10^{15}\ \text{s}^{-1}, \\
\frac{A_{\text{eff}}}{\sqrt{A_{p0} A_{s0} A_{i0}}} &= 1.33116 \times 10^{6}\ \text{m}^{-1}.
\end{aligned} \tag{S28}$$

Here, to achieve maximum effective nonlinear coefficient, we choose type-0 PDC for the largest nonlinear coefficient d_{33} = 27 pm/V [50] and poling duty cycle of 50% for the maximum Fourier coefficient, hence $\chi_{\text{eff}}^{(2)} = 2d_{33}/\pi$. Using these parameters, we calculate the relation between Q and η_{PDC} under different wavelength, which is discussed in the main text.

In order to verify our model, we compared this result with a previous work in Ref. 50, where the experimental conversion efficiency for SPDC in a LNOI microring resonator is 6.938×10^{-7}. Taking the structure of this work into our theory, the efficiency is 1.758×10^{-6}. Therefore, our theory is in good agreement with the experimental result.

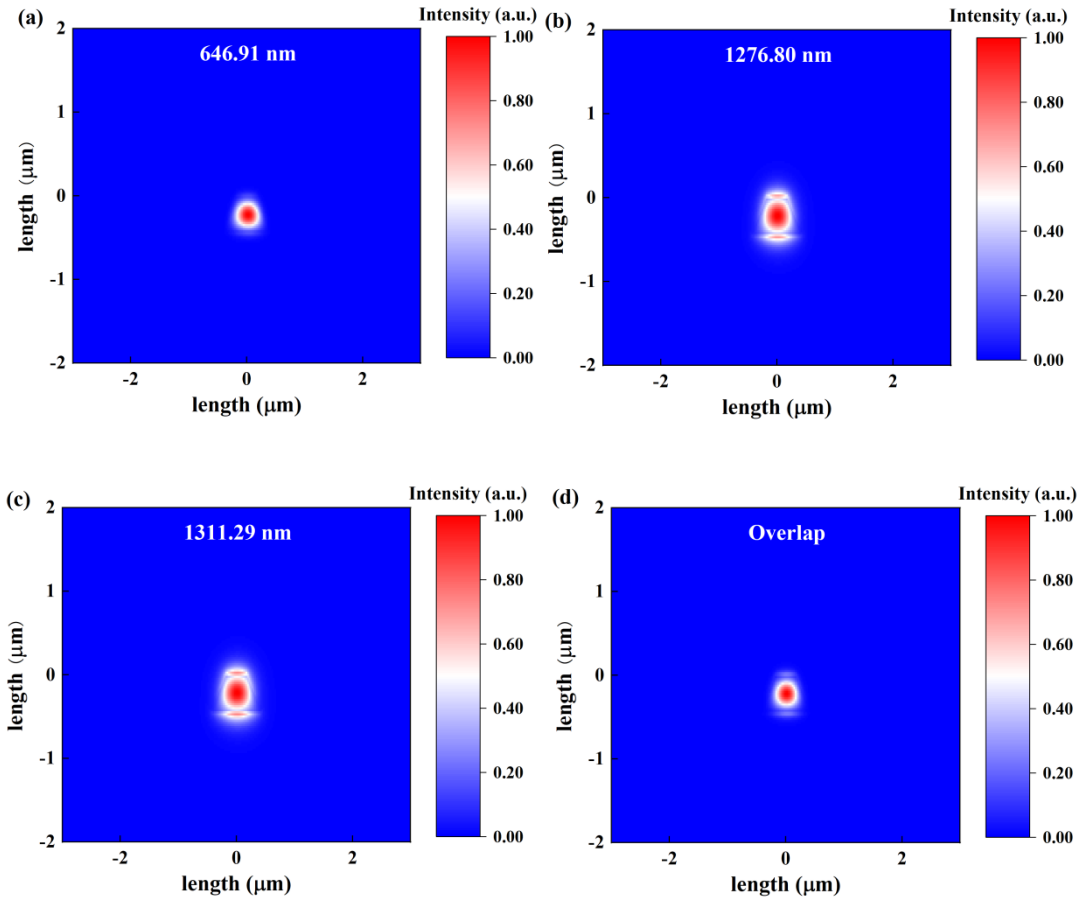

Fig. S1 The mode distribution and overlap of the three wavelengths in microring resonator waveguide: (a) 646.91 nm, (b) 1276.80 nm, (c) 1311.29 nm, (d) overlap.

Then we calculate the related parameters of the DPUC progress of 1276.80 nm (photon) + 1311.29 nm (pump laser) → 646.91 nm using PPLNOI waveguide with the same transverse structure of waveguide as the microring. The results for mode distribution and overlap of the three wavelengths is shown in Fig. S2, and the parameters are written as follows.

$$n_{646.91} = 2.058709,\ n_{1276.80} = 1.726993,\ n_{1311.29} = 1.711028,$$
$$\frac{A_{\text{eff}}}{\sqrt{A_{p0}A_{s0}A_{i0}}} = 1.332820\times10^{6}\ \text{m}^{-1}. \tag{S29}$$

Here, the effective refraction index and the overlap of the PPLNOI waveguide is slightly different from the corresponding parameters of the microring resonator, because there is no bending effect in the straight waveguide for DPUC. Using these parameters, we can calculate

the conditions for DPUC as shown in the main text.

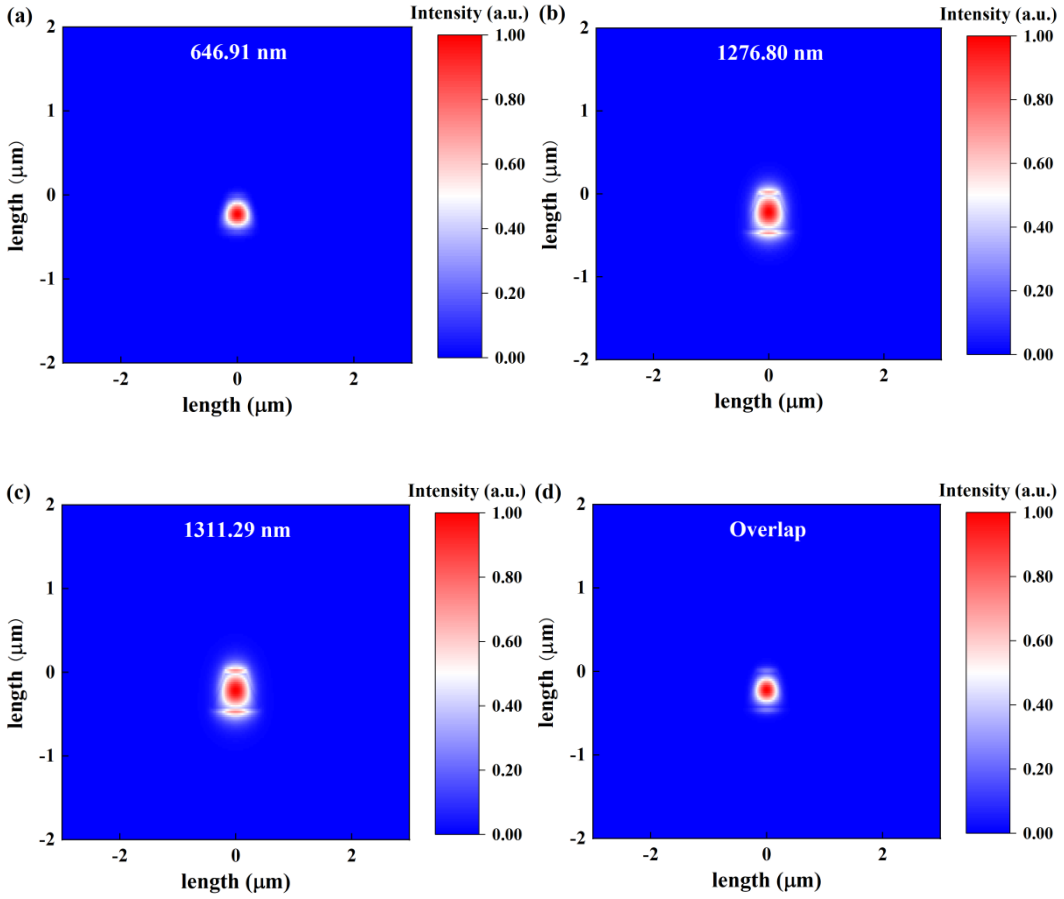

Fig. S2 The mode distribution and overlap of the three wavelengths of the straight waveguide: (a) 646.91 nm, (b) 1276.80 nm, (c) 1311.29 nm, (d) overlap.

F. Preparation of deterministic 4-photon cluster state based on PDU

In the main text, we propose an on-chip design for *N*-photon cluster states generation. Here, we take the 4-photon cluster state as an example to show the generation process in detail.

As shown in Fig. S3, we code the cluster state in path. In order to obtain the 4-photon cluster state

$$\left|\text{cluster}_4\right\rangle=\frac{1}{2}\left(\left|\tilde{0}\tilde{0}\tilde{0}\tilde{0}\right\rangle_{1234}+\left|\tilde{0}\tilde{0}\tilde{1}\tilde{1}\right\rangle_{1234}+\left|\tilde{1}\tilde{1}\tilde{0}\tilde{0}\right\rangle_{1234}-\left|\tilde{1}\tilde{1}\tilde{1}\tilde{1}\right\rangle_{1234}\right), \tag{S30}$$

one pump photon is converted to a four-photon path entanglement state through 6 PDUs and on-chip beam splitters (BS) and crossers using devices like multi-mode interference (MMI) couplers. Meantime, the relative phase of each path can be adjusted using phase modulators by devices like electro-optic modulation. Firstly, the single-photon state $\left|\mathrm{P}_{\mathrm{in}}\right\rangle$ passes through the first BS and phase plate φ_1, the state becomes $\left(\left|\mathrm{P}_{1,1}\right\rangle+e^{i\varphi_1}\left|\mathrm{P}_{1,2}\right\rangle\right)/\sqrt{2}$. Then through the PDUs connecting to input path $\mathrm{P}_{1,1}$ and $\mathrm{P}_{1,2}$, the state converts to the two-photon state $\left(\left|\mathrm{P}_{2,1}\right\rangle\left|\mathrm{P}_{2,2}\right\rangle+e^{i\varphi_1}\left|\mathrm{P}_{2,3}\right\rangle\left|\mathrm{P}_{2,4}\right\rangle\right)/\sqrt{2}$. Next, the generated photon pair interference with each other through the two BSs. After three phase plates φ_2, φ_3 and φ_4, we can get:

$$\begin{cases}\left|\mathrm{P}_{2,1}\right\rangle\rightarrow\dfrac{1}{\sqrt{2}}\left(\left|\mathrm{P}_{3,1}\right\rangle+e^{i\varphi_3}\left|\mathrm{P}_{3,3}\right\rangle\right)\\ \left|\mathrm{P}_{2,2}\right\rangle\rightarrow\dfrac{1}{\sqrt{2}}\left(e^{i\varphi_2}\left|\mathrm{P}_{3,2}\right\rangle+e^{i\varphi_4}\left|\mathrm{P}_{3,4}\right\rangle\right)\\ \left|\mathrm{P}_{2,3}\right\rangle\rightarrow\dfrac{1}{\sqrt{2}}\left(\left|\mathrm{P}_{3,1}\right\rangle-e^{i\varphi_3}\left|\mathrm{P}_{3,3}\right\rangle\right)\\ \left|\mathrm{P}_{2,4}\right\rangle\rightarrow\dfrac{1}{\sqrt{2}}\left(e^{i\varphi_2}\left|\mathrm{P}_{3,2}\right\rangle-e^{i\varphi_4}\left|\mathrm{P}_{3,4}\right\rangle\right)\end{cases}. \tag{S31}$$

Finally, via the last four PDUs with input path $\mathrm{P}_{3,1}$, $\mathrm{P}_{3,2}$, $\mathrm{P}_{3,3}$ and $\mathrm{P}_{3,4}$, we can get the 4-photon path-entangled cluster state

$$\left|\psi\right\rangle=\frac{1}{2\sqrt{2}}\begin{pmatrix}e^{i\varphi_2}\left(1+e^{i\varphi_1}\right)\left|\mathrm{P}_{4,1}\right\rangle\left|\mathrm{P}_{4,2}\right\rangle\left|\mathrm{P}_{4,3}\right\rangle\left|\mathrm{P}_{4,4}\right\rangle+e^{i\varphi_4}\left(1-e^{i\varphi_1}\right)\left|\mathrm{P}_{4,1}\right\rangle\left|\mathrm{P}_{4,2}\right\rangle\left|\mathrm{P}_{4,3'}\right\rangle\left|\mathrm{P}_{4,4'}\right\rangle\\ +e^{i(\varphi_2+\varphi_3)}\left(1-e^{i\varphi_1}\right)\left|\mathrm{P}_{4,1'}\right\rangle\left|\mathrm{P}_{4,2'}\right\rangle\left|\mathrm{P}_{4,3}\right\rangle\left|\mathrm{P}_{4,4}\right\rangle+e^{i(\varphi_3+\varphi_4)}\left(1+e^{i\varphi_1}\right)\left|\mathrm{P}_{4,1'}\right\rangle\left|\mathrm{P}_{4,2'}\right\rangle\left|\mathrm{P}_{4,3'}\right\rangle\left|\mathrm{P}_{4,4'}\right\rangle\end{pmatrix} \tag{S32}$$

The state of Eq. (S30) can be obtained if we define each pair of path qubits ($\mathrm{P}_{4,1}$ and $\mathrm{P}_{4,1'}$, $\mathrm{P}_{4,2}$ and $\mathrm{P}_{4,2'}$, $\mathrm{P}_{4,3}$ and $\mathrm{P}_{4,3'}$, $\mathrm{P}_{4,4}$ and $\mathrm{P}_{4,4'}$) as $\left|\tilde{0}\right\rangle$ and $\left|\tilde{1}\right\rangle$, and set the phase plates $\varphi_1 = \pi/2$, $\varphi_2 = 7\pi/4$, $\varphi_3 = \pi/2$ and $\varphi_4 = \pi/4$, respectively.

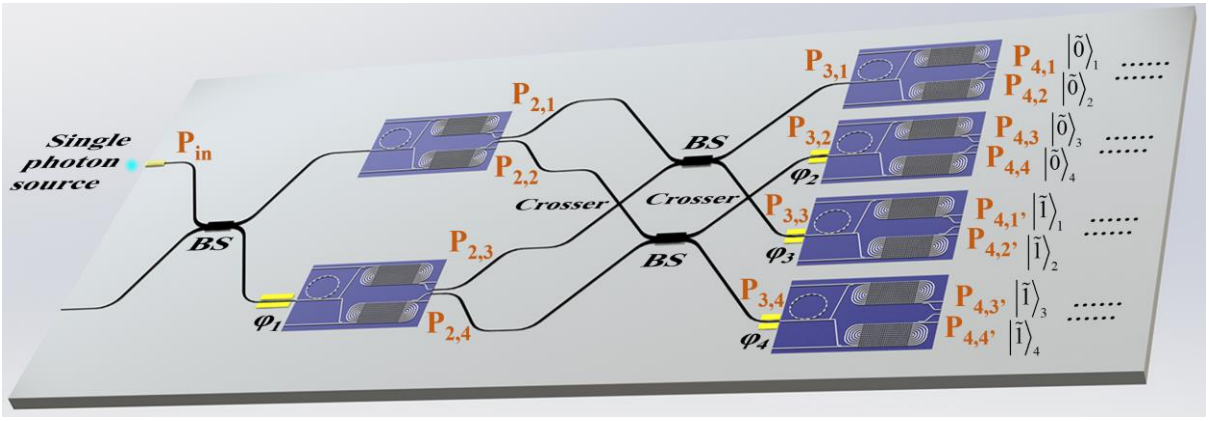

Fig. S3 Circuit design for *N*-photon cluster state, where after 2 stages, a 4-photon cluster state can be generated, in which $\varphi_1 = \pi/2$, $\varphi_2 = 7\pi/4$, $\varphi_3 = \pi/2$ and $\varphi_4 = \pi/4$.

Such module is the basic unit for large size cluster state generation. With proper design of BSs and phase plates, *N*-photon cluster states can be generated through cascading these units. Such *N*-photon cluster state is a key source for one-way computation, which is one approach for achieving universal quantum computation. After that, the only operation remaining for universal quantum computing [27, 28, 64] is single-qubit measurements of the states, which is easy to implement in optical system. [64]

G. Preparation of deterministic *N*-photon GHZ state based on PDU

Besides, we also propose an on-chip design for generation of *N*-photon GHZ state coded in path, as shown in Fig. 4(b) in the main text:

$$\left|\mathrm{GHZ}_N\right\rangle = \frac{1}{\sqrt{2}}\left(\left|\tilde{0}\right\rangle^{\otimes N} + e^{i\varphi}\left|\tilde{1}\right\rangle^{\otimes N}\right), \tag{S33}$$

Here, we also take the 4-photon GHZ state as an example. Firstly, we use a BS to convert the input single-photon Fock state $|1\rangle$ into the single-photon superposition state $\left(\left|\tilde{0}\right\rangle + e^{i\varphi}\left|\tilde{1}\right\rangle\right)/\sqrt{2}$. Then states $\left|\tilde{0}\right\rangle$ and $\left|\tilde{1}\right\rangle$ are converted to 4-photon state $\left|\tilde{0}\right\rangle^{\otimes 4}$ and $\left|\tilde{1}\right\rangle^{\otimes 4}$

respectively, through two stages of PDUs. Therefore, the final output state becomes $|\mathrm{GHZ}_4\rangle = \left(|\tilde{0}\rangle^{\otimes 4} + e^{i\varphi}|\tilde{1}\rangle^{\otimes 4}\right)/\sqrt{2}$. Following this method, *N*-photon GHZ state can be generated from single-photon superposition state $\left(|\tilde{0}\rangle + e^{i\varphi}|\tilde{1}\rangle\right)/\sqrt{2}$ followed by two groups of modules which are the same as the *N*-photon Fock state generation module, where *N* can be any positive integer bigger than 2.

H. Discussion of practical experimental factors

1. A model to analysis the influence of loss to the conversion efficiency

In the analysis of DPDC and DPUC, we assume a lossless model. Our model shows that the required Q factor of DPDC is ~4×10^7, and the intrinsic Q raised from the loss limit should be as high as possible in comparison to this number, to get high performance, especially when the system scales up. In this section, we give an estimation for the conversion efficiency with propagation loss taking into consideration.

For the DPDC process inside a microring, the nonlinear interaction time is $t_I \approx Ft_r$,[48] Correspondingly, the photons propagate through an equivalently distance of $D \approx FL$. Hence the total propagation loss would be $10^{-\kappa D/10}$, where κ is the propagation loss coefficient with unit of dB/m. Considering current material-absorption-limit Q of over 3×10^8 [57], i.e., a propagation loss of 0.119 dB/m, we estimate a total conversion efficiency of 42.2%, for a single photon to be converted to a photon pair using the PPLNOI microring. For the DPUC process, however, the propagation loss through the 10-mm waveguide is only 1.19×10^{-3} dB, which is

negligible even in a large-scale system with a few hundred steps.

The currently limit of 42.2% DPDC efficient in practice is already sufficient for the difficult task of *N*-photon state generation, and relatively large photon number generation can be expected. However, to really push towards “unitary efficiency”, the device loss needs to be further reduced. It is possible as lithium niobate is a high-transparent material, and there is no fundamental limit for reduction of the propagation loss through improving of fabrication technology, including defect and purity control during crystal growth, lattice damage control during smart cut process, and surface roughness control in the device fabrication process, etc.

2. Noise analysis in DPUC modules

Here we give a noise analysis for the DPUC process, which takes the Raman and SPDC noise in the SFG process into account. For Raman noise, since spontaneous Stokes Raman scattering is much stronger than the anti-stokes case, here we mainly calculate the Stokes Raman noise. In the straight waveguide for SFG, the Raman process is a broadband effect, so that only a very small portion of the Raman photons falls into the bandwidth in the following DPDC process, which is 5.42 MHz in our scheme. Basing on experimental result of Ref. 60, we calculate the Raman photon rate of ~0.047 Hz in our case. Such single photon counting rate from Raman noise can be well suppressed in the coincidence counting measurement when the DPDC photon rate is not too low.

The SPDC noise, on the other hand, is suppressed by the very small frequency difference between the signal and idler photons. With the proposed signal and idler wavelengths of 1276.80 nm and 1311.29 nm, the SPDC process involves a terahertz wave with wavelength of

48.5 μm. The lithium niobate and SiO_2 BOX layer are both highly absorptive, and the mode overlapping is rather small for such terahertz wave in a radiative mode.